Resonantly diode laser pumped 1.6-μm Er:YAG laser

Dmitri Garbuzov[a)] and Igor Kudryashov
Princeton Lightwave Inc., 2555 US Route 130, Cranbury, New Jersey, 08512
Mark Dubinskii
U.S. Army Research Laboratory, AMSRD-ARL-SE-EO, 2800 Powder Mill Road, Adelphi, Maryland 20783

ABSTRACT

We report what is believed to be the first demonstration of direct resonant diode pumping of a 1.6-μm Er^{3+}-doped bulk solid-state laser (DPSSL). The most of the results is obtained with pumping Er:YAG by the single mode diode laser packaged in fibered modules. The fibered modules, emitting at 1470 nm and 1530 nm wavelength with and without fiber grating (FBG) stabilization, have been used in pumping experiments. The very first results on high power DPSSL operation achieved with diode array pumping also will be presented. The highest absorbed photon conversion efficiency of 26% has been obtained for Er:YAG DPSSL using the 1470-nm single-mode module. Analysis of the DPSSL input-output characteristics suggests that the obtained slope efficiency can be increased at least up to 40% through the reduction of intracavity losses and pumping efficiency improvement. Diode pumped SSL (DPSSL) operates at a wavelength of 1617 nm. and 1645 nm

Keywords: Er:YAG , eye-safe, diode lasers.

1. INTRODUCTION

Yb:YAG solid state lasers resonantly (into the upper laser level, or Boltzmann-equilibrated neighboring levels) pumped by GaAs-diode lasers and operating at room temperature in a quasi-three level fashion demonstrate superior performance among the ~1-μm bulk solid state laser (SSL) sources [1]. This performance superiority is largely based on the low-photon-defect "pump-lase" scheme and mature technology of 940-nm Quantum Well Separate Confinement (QW SCH) lasers in the GaAs/AlGaAs or GaAs/InGaAsP systems.

Lately, impressive progress in the development of the QW SCH lasers based on InGaAsP/InP systems has been made [2-5]. Results reported in recent publications on the 1.5-μm InGaAsP/InP diode arrays [3-5] as well as on single mode lasers [2] and 1-stripe multimode emitters [3,4] have shown promising performance. For example, the output photon flux density, the key parameter for pumping applications, in case of 40-W 1.5-μm diode arrays is 50% higher than that for commercial 50-W 0.9-μm GaAs-based arrays. An outstanding feature of InGaAsP/InP-based long-wavelength pumping sources is their excellent reliability with a potential for extremely long device lifetime (~10^6 hours [2,3]).

The known shortcomings of InP-based diodes compared to GaAs diodes are reduced power conversion efficiency (30%) and higher temperature parameter sensitivity (the latter can be easily mitigated by advanced device temperature stabilization). Estimates show that reduced power conversion efficiency is going to be counter-balanced by increased optical-to-optical conversion efficiency in the case of resonantly pumped eye-safe SSL.

YAG crystal with low Er^{3+} doping is one of the most attractive active materials for developing ~1.6-μm eye-safe solid-state lasers (SSL) with resonant pumping scheme similar to that in the Yb:YAG lasers. The effectiveness of the Er^{3+}:YAG resonant pumping has been demonstrated with Er-bulk glass or Er-fiber laser pumping [6, 7]. Incident slope

Laser Source and System Technology for Defense and Security, edited by Gary L. Wood,
Proc. of SPIE Vol. 5792 (SPIE, Bellingham, WA, 2005) · 0277-786X/05/$15 · doi: 10.1117/12.603180

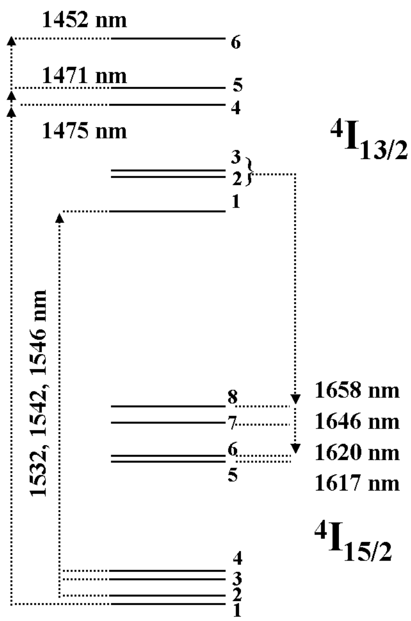

Fig.1. Er^{+3}:YAG absorptive and radiative transitions in the 1.45-1.66 μm spectral range.

efficiency as high as 54% has been achieved recently for a 1645 nm Er^{3+}:YAG laser pumped with a 1532 nm Er-fiber laser [7]. A major advantage of the InGaAsP/InP-diode-pumped Er-doped SSL laser (compared to the GaAs-diode-pumped one) is that the primary challenges of thermal management drastically shifts from Er-doped gain medium itself to the pumping diodes, thus greatly reducing gain medium thermal distortions deleterious to SSL power scaling if the diffraction-limited beam quality needs to be preserved.

Spectroscopy of the 1450-1660-nm transitions between the $^4I_{13/2}$ and $^4I_{15/2}$ Stark-split manifolds in Er^{3+}:YAG, forming a quasi-three level system (Fig.1), has been studied by several authors (e.g., [7-8]). Low-doped (0.3%<Er<2%) YAG crystals were used in [6,7,10,11] because of the strong upconversion loss in Er^{3+}:YAG at higher Er concentrations. Four upper states from the eight Stark components of the ground $^4I_{15/2}$ manifold serve as the terminal states for Er^{3+} laser transitions with the wavelengths ranging from 1617 to 1660 nm [6, 7, 10, 11].

2. PUMPING WITH SINGLE MODE DIODE LASER MODULE

2.1 Methodology.

To facilitate the first steps in this new development the high-brightness CW single-mode InP-based diode lasers were used for pumping [2]. The 1470-nm and 1530-nm ridge waveguide lasers were packaged in standard telecom 12- PIN butterfly modules with polarization maintaining fiber output. 1.6-μm lasing in Er^{3+}YAG DPSSl has been obtained with both 1530 nm and 1470 nm resonant diode pumping.

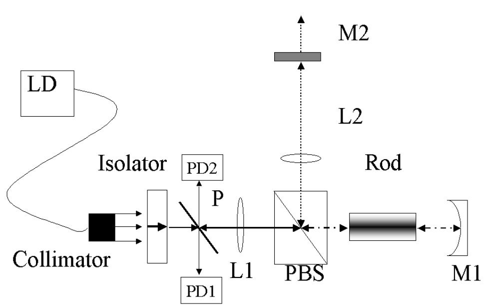

Fig. 2. Resonantly-pumped Er^{+3}:YAG DPSSL - optical layout. M_1 - plano-concave end mirror (30 mm ROC); M_2 – plano-plano output coupler; L_2 – AR-coated intracavity lens. P – diagnostic beam-splitter, PD_i - diagnostic photodiodes, LD - fiber-coupled pumping laser diode (1470 nm).

A 4.8-mm-long, 5 mm dia., Er^{3+}(1%):YAG laser rod was single-end pumped in a folded polarization-coupled cavity as shown in Fig. 2. A copper holder mounted on a thermo-electric cooler provided temperature control of the rod. A polarizing beam splitter (PBS) cube was utilized to separate pumping and lasing beam paths. Er:YAG laser confocal cavity comprised mirrors M_1 and M_2 and an AR-coated lens L_2. A lens L1 and a highly reflective concave mirror M1 (Fig. 2) provided appropriate pump volume and laser cavity mode overlap with the pump beam waist radius of about 30 μm in the rod center. Four different flat output couplers M_2 with transparencies of 0.24%, 3.3%, 9.4% and 13.9% were used in these experiments.

Two photodiodes (PD1 and PD2) and a tilted glass plate (P) shown in Fig.2, provide reference signals proportional to the incident and unabsorbed pump powers. These data acquisition system was calibrated by signals taken with no rod in the cavity. As the result, data acquisition system allowed for the effective, spectrum integrated coefficient (K_{eff}) for double-path in the rod to be measured as well as to plot the SSL output power as a function of the incident or absorbed power. Our K_{eff} measurements indicate that K_{eff} decreases as the pump power increases and also depends on the output coupler transparency. In order to quantify these phenomena, the rod absorption measurements were performed using the broadband pumping radiation as a probe.

2.2 Data and results

The data on the absorption and pumping spectrum are shown in Fig. 3. The solid curves of Fig. 3 represent the spectra of 1470 nm and 1532 nm pumping modules with and without FBG stabilization at the maximum available output powers. The pumping spectrum of the module without FBG is broadened up to 12-14 nm due to very high diode laser current density (>20 kA/cm^2). The width of the spectrum for FBG stabilized modules are comparable with spectral width of absorption lines in Er:YAG. Dashed and dotted curves of Fig. 3 display absorption spectra of Er:YAG rod measured using no-FBG modules as a source of probe radiations. These spectra were taken for the probe power at the laser threshold level (~40 mW,) as well as for the probe power level ~20 times below the threshold.

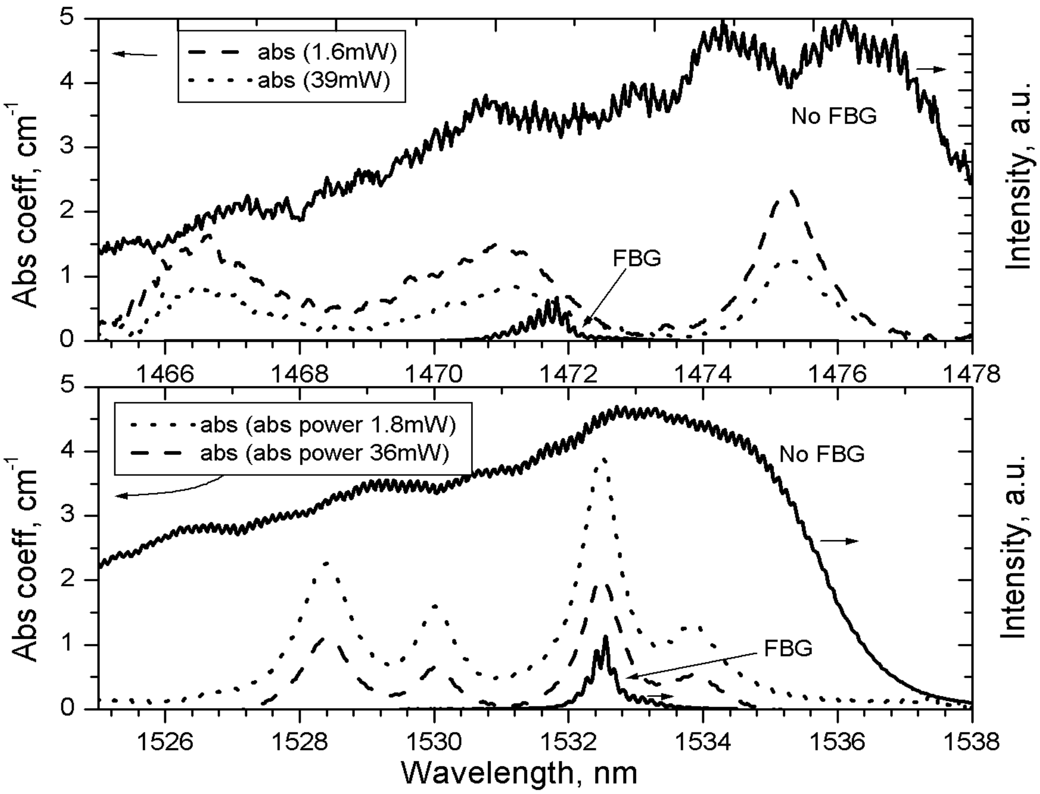

Fig. 3. The solid curves are the spectra of 1470 nm and 1532 nm pumping modules with and without FBG stabilization at the maximum available output powers. Dashed and dotted curves are absorption spectra of Er:YAG rod. Absorption curves were recorded at power levels corresponding to DPSSL threshold level (~40 mW,) and at power level ~20 times below the threshold.

It is seen that the absorption coefficient increases with probe power decrease. Further reduction of the probe density does not change the absorption. The absorption reduction observed at high probe/excitation level (bleaching effect) is taken into account during data acquisition for plotting SSL output power characteristics.

Our measurement of K_{eff} for 1530 nm pumps shows that at comparable powers K_{eff} for FBG-stabilized pump reaches 65% while it is only about 35% for pumps without FBG. The ratio of the K_{eff} values for 1470 nm pumps with and without FBG is about 1.5. Figures 4a and 4b show the DPSSL output powers as a function of the incident powers for DPSSL with 3.3% output couplers for the cases of 1530 nm and 1470 nm pumps correspondingly. Threshold incident powers are lower for FBG –stabilized pumps than that for no-FBG pumps as it is expected from comparison of the values of K_{eff} for these cases. However the slope efficiency calculated for absorbed portion of incident power are slightly higher for no-FBG pumps. We believe that this effect can be associated with fact that higher absorption coefficient for FBG-stabilized pumping radiation (up to 2 cm^{-1} for 1532 nm pump) leads to the increase of the excited Er^{3+} ion concentration gradient along rod following by the enhancement of upconversion losses , temperature gradients and thermal lensing.

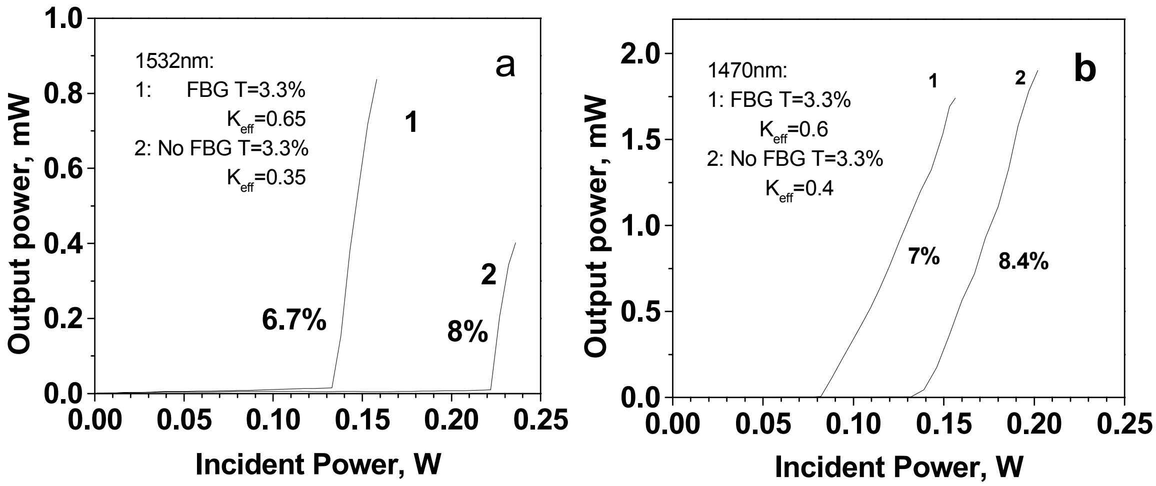

Fig 4 a and b. Input-Output characteristics for 1530 nm (a) and 1470 nm (b) single mode pumps with FBG (curves 1) and without FBG stabilization (curves 2). Slope efficiencies indicated on the graphs refer to the absorbed powers.

The dependencies of DPSSL characteristics on output coupler transparency (T) were investigated using a 1470 nm no-FBG pumping module. The bleaching effect seen from Fig. 3 explains the fact that the absorption at a fixed incident power depends on the output coupler (OC) transparency. For higher T the threshold is higher and bleaching effect is stronger. At the maximum incident power the value of K_{eff} varies with T from 45% at T=0.24% to 38% at T=13.9%. The increase in T followed by the increase in threshold also leads to the output laser spectrum variation. At T=9.4% and T=13.9% DPSSL emits single line at 1617 nm, while at T=3.3% and T=0.23% the spectrum consists of two lines - at 1617 nm and 1645 nm (Fig.5). Relative intensities of these lines do not change significantly with increasing pump power.

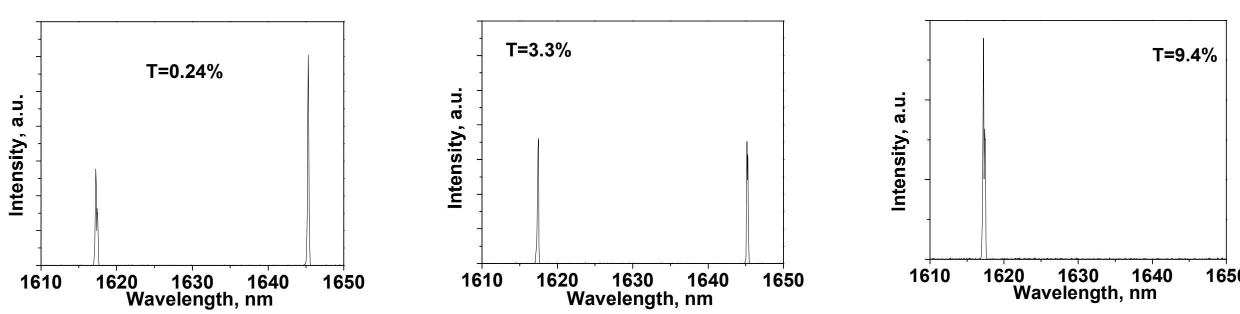

Fig. 5. DPSSL spectra for cavities with different transparencies of output couplers of 0.24%, 3.3% and 9.4%

The maximum power available from the pumping module was lower than that needed for lasing when T=13.9% at T=20 ^{0}C. The lasing with the 13.9 % coupler was achieved only after the rod temperature was reduced to 0^0 C (Fig. 6), and laser operation was restricted to only ~10% above the threshold. Nevertheless, it was possible to estimate the absorbed photon conversion efficiency (η) to be 26% ±3% (Fig. 6).

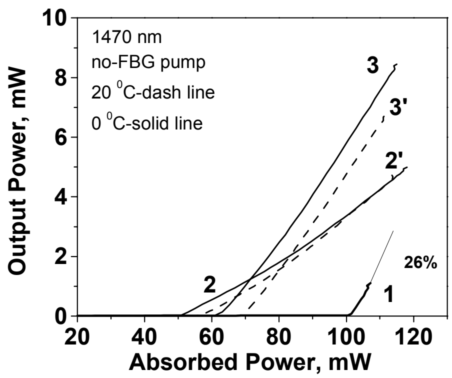

Fig. 6. Output power as a function of absorbed power for 1470-nm pumped Er^{+3}:YAG DPSSL with different output couplers: 1 - T=13.9%, 2 and 2' – T=3.3%, 3 and 3' – T=9.4%. Curves 1, 2 and 3 were measured at rod temperature 0°C and dashed curves 2′, and 3′ at 20°C.

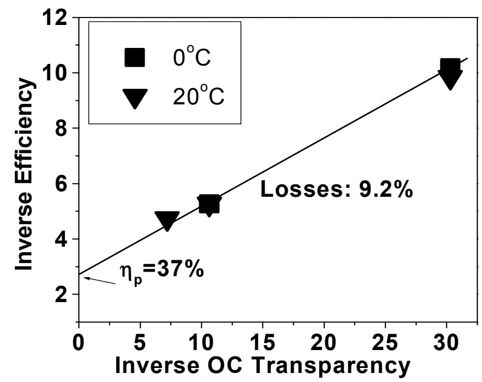

Fig. 7. Inverse absorbed photon conversion efficiency (1/η) vs. inverse output coupler transmission.

Fig. 6 displays that the cooling decreases the thresholds but does not affect the slope efficiencies of SSL**.** The data of Fig. 7 have been used to internal losses (L) and pumping coefficient (η_p) analysis, proposed by Caird [11]. By plotting these data in the format

$$\frac{1}{\eta} = \frac{1}{\eta_p}\left[1 + \frac{L}{T}\right] \qquad (1)$$

where η is the absorbed photon-to-photon conversion efficiency, intracavity losses L=9.2% and pumping efficiency η_p=0.37 were inferred (fig. 7). Obtained small value of η_p is, most likely, associated with less-than-perfect pump volume and cavity mode matching. Indirect indication of low η_p is the fact that the fluorescence intensity in non-lasing lines continues to grow with pumping above the threshold.

Direct measurements of two path absorption losses in PBS cubic at λ=1617 nm gave the value of 8%. It indicates that the intracavity losses can be reduced by an order of magnitude providing $\eta \approx \eta_p$. The pumping efficiency will also be improved substantially and in further experiments we anticipate DPSSL efficiency considerably higher than 40%.

Fig. 8 demonstrates the dependence of the absorbed power threshold on the output coupler transparency at rod temperatures of 20 ^{0}C and 0 ^{0}C. The sharp increase in the threshold power occurs at T>10%.

In order to explain this result, the intensities of the green, 1530 nm and 1617 nm fluorescence components were measured as a function of absorbed power (Fig. 9). These measurements were conducted with output coupler and in open cavity geometry without OC. 600 grooves/mm grating was used to separate spectrum florescence components. An important feature of the Fig. 9 data is the saturation of the 1617 nm and 1530 nm line intensities with pumping power increase (black and gray solid and dashed curves in Fig. 9). At pumping level close to the threshold levels the power dependencies for 1530 nm and 1617 nm lines approach $(P_p)^{1/2}$ while the dependence of the intensity of green component on pumping becomes almost linear. This fact indicates that the "bimolecular" upconversion process determines the lifetime of the excited atoms at $^4I_{13/2}$ states at threshold pumping level [11].

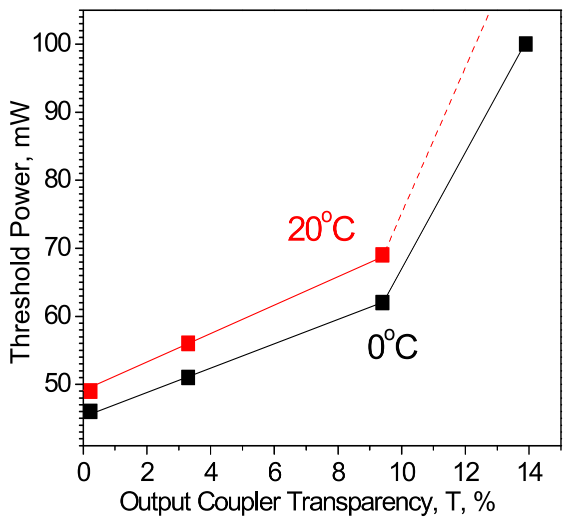

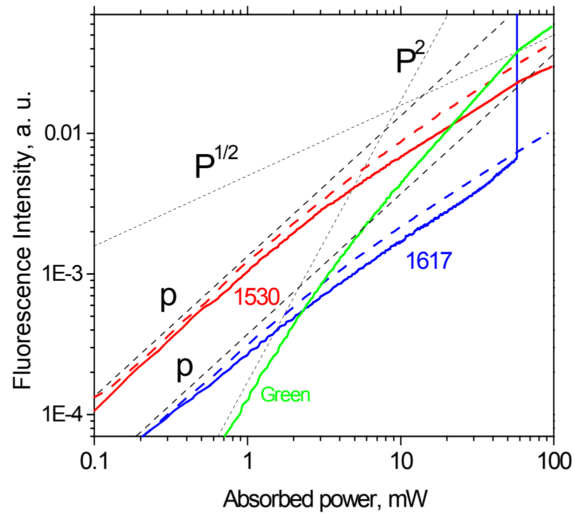

Fig. 8. Threshold absorbed power for DPSSL with different output couplers at rod temperatures 0º C and 20º C.

Fig. 9. Intensity of three fluorescence components (1617 nm, 1530 nm and green upconversion radiation) on absorbed 1475 nm power in Er(1%):YAG. Solid and dashed color lines refer to cavity with 3.3% OC and to open no-OC cavity, correspondingly. Dashed black curves are guidance lines corresponding to the linear, square and square root dependencies on power (P).

It is also seen from Fig. 9 that in the experiment with OC the 1530 nm and green fluorescence components continue to grow at pumping exceeding lasing threshold. It confirms our assumption that low value of η_p is due to non-perfect overlapping of the mode with pumped volume.

3. PUMPING WITH DIODE LASER ARRAYS.

3.1 Methodology

The results of section 2.1 indicate that for the effective absorption of pumping radiation at resonant pumping the optical path should be at least 3 cm. The modeling of values of K_{eff} for no-FBG pumps is complicated due to the bleaching effect and the difficulty of measuring low absorption coefficients between absorption lines overlapped by the pump spectrum. 3 cm long rods should have a diameter of at least 1.5-2 mm to be mechanically reliable. The pumping power (~100 W) needed for the operation of such Er:YAG DPSSL can be generated only by a diode array stack with an emitting area of about 1-2 cm^2. Simple modeling shows that it is impossible to reshape a stack radiation beam to create a pumping beam with a diameter of 2 mm and waist length of 3 cm. Our estimate for the maximum length of the waist with a diameter of 2±0.2 mm is about 0.7 cm. Therefore only the pumping scheme based on the Total Internal Reflection (TIR) approach [13] can be used for resonant diode pumping of high power Er:YAG SSL with low Er^{+3} atom concentrations.

A 3 cm long, 2 mm diameter rod with a polished barrel was used in our first TIR pumping experiment. The barrel was coated with SiO_2 and an anti-reflective coating was deposited on the end facets. A block scheme of the DPSSL is shown in Fig. 10. The pumping beam from the mini-array-stack was focused through a dichroic, 1 m radius concave mirror into the rod facet. The custom–made dichroic mirror has a transmission above 95% for 1530 nm pumping radiation and a reflectivity above 99% for 1645 nm. The DPSSL operates at 1645 nm only, because the reflectivity of this mirror decreases to 95% at 1617 nm. The linear DPSSL cavity was formed by the dichroic mirror and a plano-plano output coupler with T=9.4%.

3.2 Results

Direct measurement of the pumping power in the 2 mm aperture shows that our beam shaping optics delivers 90% of the pumping power into the rod. Ray-tracing analysis (Fig.11) demonstrates that the pumping power leakage from the barrel does not exceed 1% for an ideally polished barrel surface. Our ray-tracing modeling does not take into account the absorption in the rod so the pumping output beam keeps 99 of the 100 traced beams. Ray-tracing shows only one "leaky" beam, as seen in Fig.11. An integral measurement of post-rod pumping radiation shows that this power is 60 % lower than the incident power. The spectrum of the post-rod radiation is displayed in Fig. 12 together with the pumping spectrum.

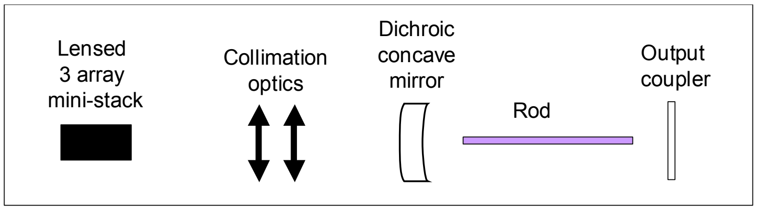

Fig. 10. Block-scheme for DPSSL with diode laser stack pumping

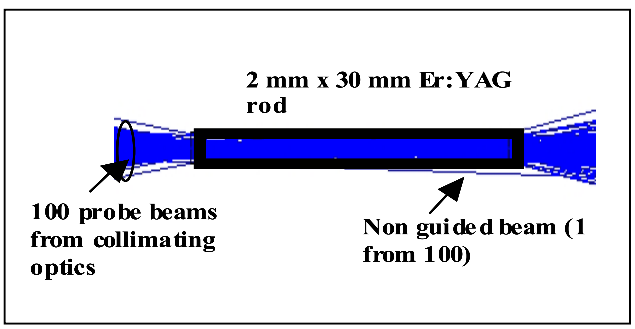

Fig. 11. The results of beam tracing analysis for 100 probe pumping beams collimated and focused by lens system into Er:YAG rod.

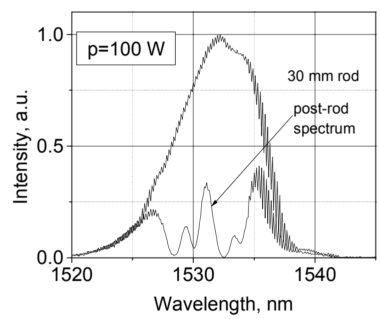

Fig. 12. The spectrum of 3 array stack at 100 W output CW power and spectrum of the post-rod pumping radiation.

These transmission measurements were performed with 90 W peak incident power. A mini-stack consisting of three 1530 nm diode arrays was used as a source of pumping radiation. The portion of the absorbed pumping radiation calculated from Fig. 12 is slightly higher (≅70%) than the results of direct integral absorption measurements.

In these first experiments with array stack pumping, our attention was focused on the pumping radiation absorption and on the distribution of the excited Er^{+3} ions along the rod. In order to perform these measurements the rod was not fixed to the copper heatsink but lying in the copper groove with the top portion of the barrel exposed. This allowed us to measure the distribution of the green upconversion radiation along the rod. A CCD camera was used for this purpose. As seen in Fig. 13, even at the maximum incident power of 90 W, the green radiation intensity was four times weaker near the output rod end than near the front pumped end. The gradient in the intensity of green fluorescence is greater at the near threshold incident power level of 54 W.

Gradient of gain/absorption along the rodincreases the threshold and decreases the DPSSL efficiency due to thermal lensing. As seen from Fig. 14, the lasing pulse intensity does not reach a stationary value and starts to decrease after 6 ms after the beginning of the 15 ms pumping radiation pulse. Because of this, the slope efficiency for absorbed pump radiation is only 15-10% and 1645 nm peak pulse power is only 3.3 W at 60 W absorbed pumping power. The absorbed power at the threshold is about 30 W. Further experiments with the rod fixed to the copper heatsink will allow us to determine other factors limiting the output power of the array pumped DPSSL.

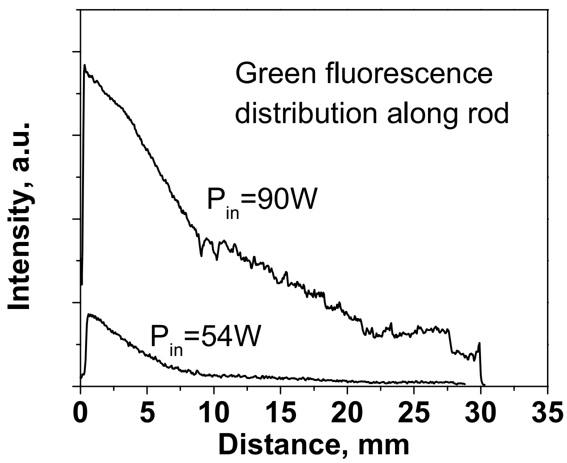

Fig. 13. Distribution of green fluorescence along 30 mm long Er: YAG at 1530 nm diode stack pumping at near threshold (54 W) and above threshold (90) W incidents powers.

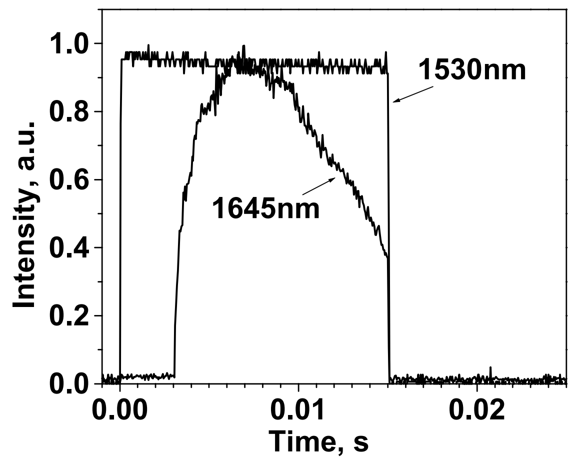

Fig. 14. Shapes of the pumping pulse and lasing pulse of DPSSL

4. CONCLUSION.

In this work, the resonant diode pumping has been demonstrated for the eye-safe Er: YAG solid state laser (SSL). The fibered diode laser modules, emitting at 1470 nm and 1530 nm wavelength and 1530 nm diode arrays have been used as the pumping sources. Diode pumped SSL (DPSSL) operates at a wavelength of 1617 nm and 1645 nm.

The lowest threshold for incident power was observed for DPSSL pumped with FBG- stabilized modules due to high absorption for pumping radiation. FBG-assisted pumping can be applied in the development of miniature portable eye-safe Q-switch DPSSL. DPSSL with non-FBG pumping demonstrated the absorbed photon conversion efficiency as high as 26%. Analysis of the DPSSL output characteristics indicates that obtained slope efficiency can be doubled through the reduction of an intercavity losses and pumping efficiency improvement.

Measurements of infrared and green fluorescence intensities demonstrated that the upconversion becomes the dominant recombination mechanism determining lifetime of excited $^4I_{13/2}$ states in Er(1%): YAG at the pumping levels corresponding to the lasing thresholds. It leads to the super linear increase of the pumping threshold with increase of the output losses. Data on the upconversion impact are essential for low threshold Er^{3+}:YAG DPSSL design.

First experiments with diode array stack were focused on the effective coupling of the pumping radiation into the rod with length large enough for effective absorption of the broad wavelength pump radiation.

Modeling and experiments demonstrated that 90% of pumping radiation from 1530 nm single diode array or array stack can be coupled in 2 mm diameter 3 cm long Er:YAG rod without duct implementation.. TIR approach for pumping provides leakage losses <0.2% for pump radiation coupled from the array stack to the front rod end. 3.3 W peak power from DPSSL with 2mm x 30 mm rod has been obtained in the first experiments with 10 ms pump pulses.

This work was supported by the HEL-JTO/AF through the BAA Contract No.: FA9451-04-C-0189

REFERENCES

1. W. F. Krupke, Ytterbium solid-state lasers. The first decade. - IEEE J. of Sel. Top. Quant. Electron. **6** (6), 1287–1296 (2000).
2. D. Garbuzov, I. Kudryashov, A. Komissarov, M. Maiorov, W. Roff, and J. Connolly "High Power Raman Pumps Based on Ridge Waveguide InGaAsP/InP Diode Lasers" in Technical Digest of OFC 2003, (OSA, 2003), pp 10-12
3. D. Garbuzov, M. Dubinskii, "InP-based Long Wavelength Sources for Solid State Diode Pumping," in Technical Digest of Solid State and Diode Lasers Technology Review, SSDLTR 2004, Direct Energy Professional Society, p-19.
4. P. Crump, T. Crum, M. DeVito, J. Farmer, M. Grimshaw, Z. Huang, S. Igl, J. Wang, W. Dong, "High Power 1470 nm Laser Bars and Stacks," Technical Digest of SSDLTR 2004, Direct Energy Professional Society, Diode-3.
5. R. Lammert, M. Osowski, M. Young, S.Oh, J. Ungar, "Laser Diodes Bars with High Efficiency at high Temperature," in Technical Digest of Solid State and Diode Lasers Technology Review, SSDLTR, 2004, Direct Energy Professional Society, P-10
6. K. Spariosu, M. Birnbaum. IEEE J. Quant. Electron., "Intracavity1.549 μm pumped 1634 μm Er:YAG laser", **30**, p.1044, (1994).
7. Y. Young, S. Setzler, K. Snell, P. Budni, T. Polak, E. Chiklis, "Efficient 1645 nm Er:YAG Laser," Optics Letters, **29**, p 1075, (2004)
8. N. Agladze, M. Popova, E. Vinogradov, T. Murina, V. Zhekov, Opt. Commun."Oscillator Strength in$Y_3A_{l5}0_{12}$-Er^{+3}," **65**, p 351, (1988)
9. T. Schweizer, T Jensen, E. Heumann, G. Huber, Opt. Commun.,"Spectroscopic Properties of Yb: Er:YAG," **118**, p. 557, (1995)
10. H. Stange, K. Petermann, G. Huber, E. Duczynski, "CW 1.6 μm Laser Action in Er:YAG," Appl. Phys. **B 49**, p. 269, (1989)
11. M. Iskandarov, A. Nikitichev, A. Stepanov, "Quasi-two-level Er:YAG laser for 1.6 μm range," J. Opt. Technol., **68(12), p.** 885,(2001)
12. J. Caird, S. Payne, P. Staver, A. Ramponi, L. Chase, W. Krupke, "Quantum Electronics Properties of the NaGaLiF:Cr^{3+}", IEEE J.Quantum Electronics, **QE-24**, p. 1077, (1988
13. C. Bibeau, R. Beach, S. Mitchell, M. Emanuel, J. Skidmore, C. Ebbers, S. Sutton, K. Jancaitis, "High-Average-power 1-μm Performance and Frequency Conversion of a Diode-End-Pumped Yb:YAG Laser", IEEE J. Quantum Electronics, **QE-34**, p.2010, (1998)